View Article Online / Journal Homepage / Table of Contents for this issue



# Nickel(II) complexes of cyclen- and cyclam-pyridine: topological reorganisations induced by electron transfer†

**Sanae El Ghachtouli,[a] Cyril Cadiou,[a] Isabelle Déchamps-Olivier,[a] Françoise Chuburu,*[a] Michel Aplincourt,[a] Véronique Patinec,[b] Michel Le Baccon,[b] Henri Handel[b] and Thierry Roisnel[c]**

***Received (in Montpellier, France) 24th October 2005, Accepted 19th December 2005***
***First published as an Advance Article on the web 20th January 2006***
**DOI: 10.1039/b515107d**

Downloaded by University of California - Los Angeles on 01 January 2013
Published on 20 January 2006 on http://pubs.rsc.org | doi:10.1039/B515107D

The $Ni^{II}$ complexes of cyclen- and cyclam-pyridine (respectively 1-pyridin-2-ylmethyl-1,4,7,10-tetraazacyclododecane and 1-pyridin-2-ylmethyl-1,4,8,11-tetraazacyclotetradecane denoted $[Ni^{II}L^1]^{2+}$ and $[Ni^{II}L^2]^{2+}$) have been isolated and characterised by X-ray diffraction, UV-visible spectroscopy and electrochemical studies for the $[Ni^{II}L^2]^{2+}$ complex. In particular, the $[Ni^{II}\ L^2]^{2+}$ complex adopts two distinct and stable geometries (type I and V), which mainly differ by the macrocycle configuration. In solution, the isomerisation process between these two configurations is driven by the nickel-centered electron transfer.

## Introduction

Macrocyclic polyamines, like cyclen or cyclam, bearing coordinating pendant arms have attracted a lot of attention[1] since they can be involved in numerous fields ranging from diagnostic and nuclear medicine[2] to waste-water treatment.[3] Generally, the additional donor groups of the pendant arms improve the thermodynamic and the kinetic stability of the metallic complex. This property is crucial in particular for medical purposes since the *in vivo* metal release must be strictly avoided. A good example to illustrate this aspect is the coordination of the $Gd^{III}$ cation by the tetraacetate cyclen ligand: the corresponding $[Gd(DOTA)H_2O]^-$ complex is currently one of the most stable and inert gadolinium complexes known and administered for MRI examinations.[4]

Beside these considerations, complexes of such ligands show interesting structural features since the functionalised side arms can coordinate and stabilise the metal centre. Furthermore, if the side chain presents a donor group (for example an amine), its coordination may be tuned according to the pH for instance.[5] Thus, at acidic pH, the proton and the metal ion compete with each other because if the donor group of the side chain is protonated it can no longer interact with the metal ion in the macrocycle. Another way to induce modifications in the metal coordination shell is to modify the metal redox state. This aspect is certainly worth investigating since it can lead to molecular switches for molecular electronics, multiredox activity, catalysis or biomimetic chemistry.[6] Unlike copper complexes,[7] relatively few investigations have described the effects of the redox processes on structural rearrangements of nickel complexes.[8] In this work, besides the effect of the pH on the coordination of a pyridine pendant arm on complexes of cyclen- and cyclam-pyridine (respectively denoted $[Ni^{II}L^1]^{2+}$ and $[Ni^{II}L^2]^{2+}$ Scheme 1), an investigation of the electrochemical behaviour of $[Ni^{II}L^2]^{2+}$ complex is undertaken to demonstrate that the application of a redox stimulus induces reversible rearrangements between distinct geometries of the complex in solution. These experiments are furthermore supported by the X-ray identification of the configurational isomers.

## Results and discussion

### Synthesis and structural characterisation in the solid state of complexes $[Ni^{II}L^{1,2}]^{2+}$

The ligands $\mathbf{L^1}$ and $\mathbf{L^2}$ were prepared following the bis(aminal) methodology[9] and the corresponding Ni(II) metal complexes were synthesised by reacting stoichiometric amounts of ligand and metal salt in methanol.

The X-ray structure of the $[Ni^{II}L^1]^{2+}$ complex shows that the geometry around the nickel ion is octahedral (Fig. 1, Table 1). The structure clearly demonstrates a *cis* folded $N_4$ configuration of the cyclen cavity so that the pyridine ring and an acetonitrile molecule can be accommodated in *cis* positions. Three nitrogen atoms of the macrocycle [$d_{Ni-N_1}$ = 2.117(2) Å,

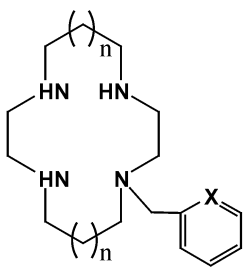


$n = 0$, $\mathbf{X = N : L^1}$
$n = 1$, $\mathbf{X = N : L^2}$
$n = 1$, $\mathbf{X = CH : L^3}$

**Scheme 1**

[a] *GRECI, Université de Reims Champagne-Ardenne, BP 1039, 51687 REIMS Cedex 2, France. E-mail: francoise.chuburu@univ-reims.fr*
[b] *Chimie, Electrochimie moléculaires et chimie analytique, UMR CNRS 6521, Université de Bretagne Occidentale, CS 93837, 29285 BREST Cedex, France*
[c] *Institut de Chimie de Rennes, UMR CNRS 6511, CS 74205, 35042 RENNES Cedex, France*

† Electronic supplementary information (ESI) available: UV-visible absorption spectra and cyclic voltammograms of the nickel(II) complexes. See DOI: 10.1039/b515107d

 This journal is © the Royal Society of Chemistry the Centre National de la Recherche Scientifique 2006

Downloaded by University of California - Los Angeles on 01 January 2013
Published on 20 January 2006 on http://pubs.rsc.org | doi:10.1039/B515107D

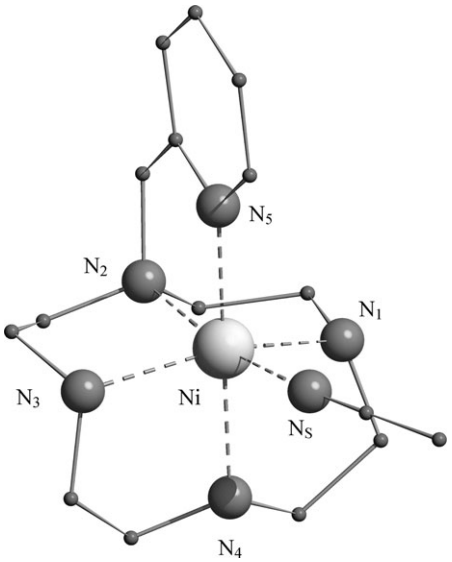


**Fig. 1** Schakal diagram of $[NiL^1]^{2+}$.

$d_{Ni-N_2}$ = 2.140(2) Å, $d_{Ni-N_3}$ = 2.117(2) Å] and the nitrogen atom of an acetonitrile molecule [$d_{Ni-N_S}$ = 2.084(2) Å] coordinate in a square planar fashion while the nitrogen pyridine atom [$d_{Ni-N_5}$ = 2.083(2) Å] and the remaining $N_4$ of cyclen [$d_{Ni-N_4}$ = 2.111(2) Å] bind apically.

In the course of the $[Ni^{II}L^2]^{2+}$ synthesis, two solids were obtained and crystallised. The first one precipitates in the solution and light pink crystals were grown from acetonitrile–ether to give the $[Ni^{II}L^2(CH_3CN)]^{2+}$ complex (Fig. 2a, Table 2a). The second one $[Ni^{II}L^2(H_2O)]^{2+}$ is purple and is obtained by slow evaporation of the native supernatant solution (Fig. 2b, Table 2b). $[Ni^{II}L^2(CH_3CN)]^{2+}$ and $[Ni^{II}L^2(H_2O)]^{2+}$ in the solid state differ mainly by the relative position of the solvent molecule in the metal coordination sphere and then by the configuration of the cyclam moiety. In these stereoisomers, the cyclam configuration can be described according to the well-known nomenclature developed by Bonisch and co-workers.[10] According to this classification, the $[Ni^{II}L^2(CH_3CN)]^{2+}$ complex (Fig. 2a) adopts a type I (*RSRS*) configuration. Despite the poor quality of the diffraction data and structure refinement (crystals are not so stable out of the crystallisation solution) one can see that the nickel environment is provided by the four coplanar nitrogen atoms of the cyclam moiety and the nickel stays in this plane. Moreover, the nitrogen pyridine

**Table 1** Selected bond lengths (Å) and angles (°) in $[NiL^1(CH_3CN_{(S)})]^{2+}$

| | | | |
|---|---|---|---|
| Ni–$N_1$ | 2.117(2) | Ni–$N_2$ | 2.140(2) |
| Ni–$N_3$ | 2.117(2) | Ni–$N_4$ | 2.111(2) |
| Ni–$N_5$ | 2.083(2) | Ni–$N_S$ | 2.084(2) |
| | | | |
| $N_1$–Ni–$N_2$ | 83.51(7) | $N_1$–Ni–$N_3$ | 156.00(7) |
| $N_1$–Ni–$N_4$ | 81.63(7) | $N_1$–Ni–$N_5$ | 101.48(7) |
| $N_1$–Ni–$N_S$ | 94.59(7) | $N_2$–Ni–$N_3$ | 84.05(7) |
| $N_2$–Ni–$N_4$ | 104.01(8) | $N_2$–Ni–$N_5$ | 80.88(8) |
| $N_2$–Ni–$N_S$ | 170.79(8) | $N_3$–Ni–$N_4$ | 81.59(7) |
| $N_3$–Ni–$N_5$ | 96.69(7) | $N_3$–Ni–$N_S$ | 100.76(7) |
| $N_4$–Ni–$N_5$ | 174.56(8) | $N_4$–Ni–$N_S$ | 84.57(8) |
| $N_5$–Ni–$N_S$ | 90.71(8) | | |

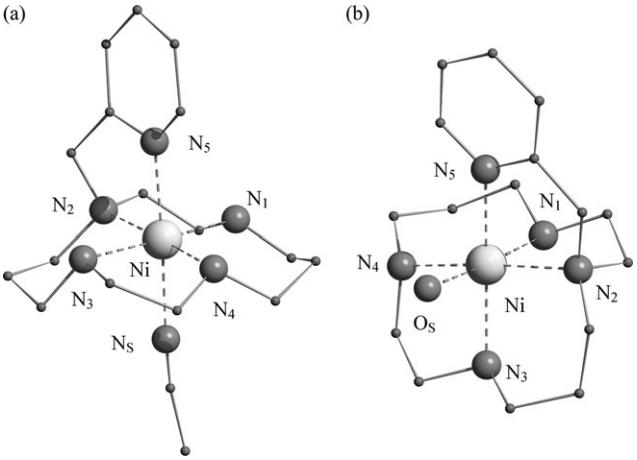


**Fig. 2** (a) Schakal diagram of $[NiL^2]^{2+}$-type I; (b) Schakal diagram of $[NiL^2]^{2+}$-type V.

atom ($N_5$) is bound apically ($d_{Ni-N_5}$ = 2.107 Å) while the second apical position is occupied by an acetonitrile molecule.

For the $[Ni^{II}L^2(H_2O)]^{2+}$ complex (Fig. 2b), one can identify the structure as the less common type V (*RRRR*) configuration.[11] The complex exhibits a *cis* folded $N_4$ configuration for cyclam. As for the cyclen analogue, three nitrogen atoms of the macrocycle ($N_1$, $N_2$, $N_4$) and a water molecule are coordinated in a square planar fashion while the nitrogen atom of the pyridine and the remaining $N_3$ nitrogen atom of the macrocycle bind apically. It is well known that for nickel(II) cyclam complexes, the type V (*RRRR*) diastereoisomer is the less stable. In our context, the six-coordinated type V (*RRRR*)

**Table 2** Selected bond lengths (Å) and angles (°) in (a) $[NiL^2(CH_3CN_{(S)})]^{2+}$-type I and (b) $[NiL^2(H_2O_{(S)})]^{2+}$-type V

a

| | | | |
|---|---|---|---|
| Ni–$N_1$ | 2.058(13) | Ni–$N_2$ | 2.158(13) |
| Ni–$N_3$ | 2.005(11) | Ni–$N_4$ | 2.065(12) |
| Ni–$N_5$ | 2.107(10) | Ni–$N_S$ | 2.216(10) |
| | | | |
| $N_1$–Ni–$N_2$ | 84.1(6) | $N_1$–Ni–$N_3$ | 171.9(6) |
| $N_1$–Ni–$N_4$ | 99.4(5) | $N_1$–Ni–$N_5$ | 89.0(5) |
| $N_1$–Ni–$N_S$ | 88.3(5) | $N_2$–Ni–$N_3$ | 88.1(7) |
| $N_2$–Ni–$N_4$ | 176.5(6) | $N_2$–Ni–$N_5$ | 80.0 (4) |
| $N_2$–Ni–$N_S$ | 93.0(4) | $N_3$–Ni–$N_4$ | 88.4(6) |
| $N_3$–Ni–$N_5$ | 91.9(4) | $N_3$–Ni–$N_S$ | 89.9(4) |
| $N_4$–Ni–$N_5$ | 100.4(4) | $N_4$–Ni–$N_S$ | 86.8(4) |
| $N_5$–Ni–$N_S$ | 172.7(5) | | |

b

| | | | |
|---|---|---|---|
| Ni–$N_1$ | 2.099(3) | Ni–$N_2$ | 2.141(3) |
| Ni–$N_3$ | 2.091(3) | Ni–$N_4$ | 2.131(3) |
| Ni–$N_5$ | 2.109(3) | Ni–$O_S$ | 2.213(3) |
| | | | |
| $N_1$–Ni–$N_2$ | 84.62 (14) | $N_1$–Ni–$N_3$ | 97.74 (14) |
| $N_1$–Ni–$N_4$ | 89.59 (13) | $N_1$–Ni–$N_5$ | 92.83 (13) |
| $N_1$–Ni–$O_S$ | 176.00 (13) | $N_2$–Ni–$N_3$ | 92.37 (14) |
| $N_2$–Ni–$N_4$ | 172.24 (14) | $N_2$–Ni–$N_5$ | 81.95 (13) |
| $N_2$–Ni–$O_S$ | 94.15 (14) | $N_3$–Ni–$N_4$ | 83.26 (15) |
| $N_3$–Ni–$N_5$ | 167.50 (15) | $N_3$–Ni–$O_S$ | 86.11 (13) |
| $N_4$–Ni–$N_5$ | 103.56 (13) | $N_4$–Ni–$O_S$ | 91.96 (13) |
| $N_5$–Ni–$O_S$ | 83.22 (13) | | |

View Article Online

Downloaded by University of California - Los Angeles on 01 January 2013
Published on 20 January 2006 on http://pubs.rsc.org | doi:10.1039/B515107D

**Table 3** Electronic data in aqueous and acetonitrile solutions

| $\lambda$ (nm) [$\varepsilon$ ($mol^{-1}$ L $cm^{-1}$)] | $H_2O$ | $CH_3CN$ | $HClO_4$ (5 mol $L^{-1}$) |
|---|---|---|---|
| $[Ni^{II}L^1]^{2+}$ | 839 [20], 540 [11] | 856 [20], 522 [15], 320 | 385 [9] |
| $[NiL^2]^{2+}$-type I | 782 [11], 513 [38] | 490 [22], 337 [82] | 455 [7] |
| $[NiL^2]^{2+}$-type V | 876 [23], 523 [30] | 842 [8], 524 [9], 306 [85] | 455 [7] |
| Chromophore[a] | $NiN_5S$ | $NiN_5S$ | $NiN_4$ |

[a] S = $H_2O$ or $CH_3CN$.

$[Ni^{II}L^2(H_2O)]^{2+}$ complex is stabilised and it can be correlated, as suggested by molecular mechanics calculations,[12] to the Ni–N distances $>ca.$ 2.10 Å (Ni–$N_5$ included). Finally, for both isomers, most of the Ni–N bond distances are in the 2.05 to 2.10 Å range, as expected for high-spin Ni(II)–N bonds.[11]

### Electronic absorption spectroscopy

In order to check whether the nickel coordination sphere is modified for the complexes in solution, UV-visible absorbance spectra of $[Ni^{II}L^1]^{2+}$, $[Ni^{II}L^2]^{2+}$-type I and $[Ni^{II}L^2]^{2+}$-type V were recorded in water and acetonitrile (Table 3).†

For the cyclen complex $[Ni^{II}L^1]^{2+}$, the UV-visible spectrum is indicative of an octahedral coordination for nickel. Two bands are observed for both complexes whatever the solvent, corresponding to the predicted $^3A_{2g} \rightarrow {}^3T_{2g}$ (839 nm in water and 856 nm in $CH_3CN$) and $^3A_{2g} \rightarrow {}^3T_{1g}$ (F) (540 nm in water and 522 nm in $CH_3CN$) transitions for a $d^8$ metal ion in an octahedral environment, the third transition $^3A_{2g} \rightarrow {}^3T_{1g}$ (P) (320 nm) being partially hidden by the stronger absorbance of the ligand ($\lambda < 300$ nm). For this complex, the octahedral nickel environment is maintained in solution, the pyridine nitrogen atom and one molecule of solvent occupying the two last positions of the octahedron.[13,14]

For the cyclam $[Ni^{II}L^2]^{2+}$-type I and $[Ni^{II}L^2]^{2+}$-type V complexes, the UV-visible spectra exhibit the same features as the cyclen one whatever the solvent. For instance in water, the $[Ni^{II}L^2]^{2+}$-type I complex exhibits two bands of weak intensity at 782 and 513 nm, the third expected one being hidden by the absorbance of the ligand ($\lambda < 300$ nm). $[Ni^{II}$(cyclam)] complex is known to exist as a mixture of square planar and octahedral species according to the following solvent (S) equilibrium.[15]

$$[Ni^{II}L]^{2+} + 2S \rightleftharpoons [Ni^{II}L(S)_2]^{2+}$$

square planar — low - spin ⇌ octahedral — high - spin

In our case, as well as in water or acetonitrile, the absorption band of the square planar form is absent (a more intense band than the octahedral ones, is expected at 400–450 nm), one can conclude that the $[Ni^{II}L^2]^{2+}$ cyclam complexes exist in solution in the octahedral high-spin form. In these conditions, for both complexes $[Ni^{II}L^2]^{2+}$-type I and $[Ni^{II}L^2]^{2+}$-type V, the pyridine nitrogen atom remains coordinated to the nickel ion in solution. This can easily be proved in aqueous solution since the addition of $HClO_4$ (5 mol $L^{-1}$) induces, for both complexes, the disappearance of the bands of the octahedral system in favour of a single intense absorption at about 455 nm.[16] As described for the parent $[Ni^{II}$(cyclam)$]^{2+}$, this band is characteristic of a square planar system where the nitrogen pyridine atom is no longer coordinated to the nickel ion. It is noticeable that only a strong acid medium is able to protonate the nitrogen pyridine atom and then to remove it from the metal.

### Redox properties of the nickel cyclam complexes

The cyclen cavity is not well adapted to stabilise +I and +III oxidation states for nickel.[17] Therefore it was not possible to obtain reproducible voltammograms, mainly due to the degradation of oxidised and reduced forms during the experiment.

Concerning the cyclam complexes, X-ray data show that the two complexes differ in the stereochemistry at the coordinated nitrogens and this difference may influence the redox potentials of the species. In this condition, it is important to consider the consequence of the complex structures on the redox potentials. Furthermore, the redox stimulus influence on the isomerisation process of nickel cyclam complexes needs to be observed more closely. Some examples of configurational isomerisation for copper cyclam complexes consecutive to the metal redox state modification are known[7] but equilibria on mono-N-functionalised nickel cyclam complexes are scarce,[8a,14] in particular between type V/I configurations. For that, the ability to trigger a movement between $[Ni^{II}L^2]^{2+}$ complexes was judged from cyclic voltammetry experiments.

Measurements were carried out first in an $Na_2SO_4$ 0.5 mol $L^{-1}$ aqueous solution,[18] the working electrode being a glassy carbon disk, the reference a saturated calomel electrode (potassium chloride) and the counter electrode a platinum rod. The $Ni^{II/III}$ half wave potentials are collected in Table 4. The oxidation of $[Ni^{II}L^2]^{2+}$-type I is quasi-reversible and occurs at 0.64 V *vs.* SCE (Fig. 3a). The oxidation of $[Ni^{II}L^2]^{2+}$-type V (1.00 V *vs.* SCE) is irreversible and leads after 40 scans at 100 mV $s^{-1}$ or 15 min of electrolysis at 1.10 V *vs.* SCE to the unique formation of the $[Ni^{II}L^2]^{2+}$-type I system (Fig. 3b). Therefore, one can think that the $[Ni^{III}L^2]^{3+}$-type V complex formed by oxidation is unstable and quickly isomerises into the $[Ni^{III}L^2]^{3+}$-type I cation for

**Table 4** Half wave oxidation potentials of $[Ni^{II}L^2]^{2+}$-type I, $[Ni^{II}L^2]^{2+}$-type V and $[Ni^{II}L^3]^{2+}$-type III in aqueous medium ($Na_2SO_4$, 0.5 mol $L^{-1}$ or $HClO_4$ 5 mol $L^{-1}$)

| Complex | Medium | $E_{\frac{1}{2}}^{ox}$ (V) *vs.* SCE |
|---|---|---|
| $[Ni^{II}L^2]^{2+}$-type I | $Na_2SO_4$ 0.5 mol $L^{-1}$ | 0.64 ($\Delta E_p$ = 100 mV) |
| $[Ni^{II}L^2]^{2+}$-type V | $Na_2SO_4$ 0.5 mol $L^{-1}$ | $E_p^{ox}$ = 1.00 (irrev.) |
| $[Ni^{II}L^2]^{2+}$-type I | $HClO_4$ 5 mol $L^{-1}$ | 0.72 ($\Delta E_p$ = 100 mV) |
| $[Ni^{II}L^3]^{2+}$-type III | $Na_2SO_4$ 0.5 mol $L^{-1}$ | 0.72 ($\Delta E_p$ = 100 mV) |

 This journal is © the Royal Society of Chemistry the Centre National de la Recherche Scientifique 2006

Published on 20 January 2006 on http://pubs.rsc.org | doi:10.1039/B515107D
Downloaded by University of California - Los Angeles on 01 January 2013

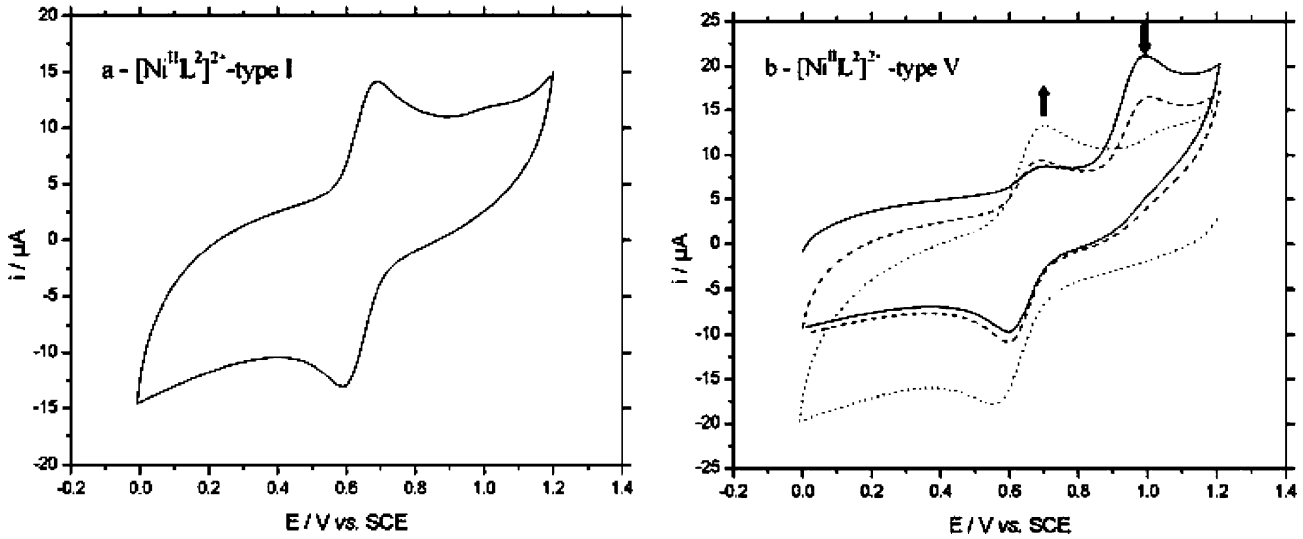


**Fig. 3** Cyclic voltammetry at a glassy carbon disk (100 mV $s^{-1}$) in an $Na_2SO_4$ 0.5 mol $L^{-1}$ solution of (a) $[Ni^{II}L^2]^{2+}$-type I and (b) $[Ni^{II}L^2]^{2+}$-type V (first scan in solid line, dashed line after 5 scans and dotted line after a 15 min electrolysis at 1.10 V *vs.* SCE or 40 scans).

which the $E_{\frac{1}{2}}$ potential is estimated at 0.64 V *vs.* SCE. From this observation, it is possible to build the following square scheme involving the oxidatively induced isomerisation of the type V to the type I isomers (Scheme 2).[19] In this reaction scheme, isomerisation between type I and type V isomers at their +II oxidation state is also involved. This point is supported by the fact that when a type I aqueous solution is kept for about seven days at room temperature, its first oxidation scan shows a small wave at 1.00 V (type V) *vs.* SCE, which tends to disappear after several scans in favour of the type I system. This seems to indicate that the equilibrium between $[Ni^{II}L^2]^{2+}$-type I and $[Ni^{II}L^2]^{2+}$-type V is shifted towards the type I isomer. Another way to confirm the isomerisation of $[Ni^{III}L^2]^{3+}$-type V into $[Ni^{III}L^2]^{3+}$-type I in aqueous medium is to perform a chemical oxidation of the $Ni^{II}$-type V isomer. This was made using half an equivalent of $(NH_4)_2S_2O_8$ at pH = 7 and the corresponding $Ni^{III}$ sample shows a voltammetry typical of the type I complex in $Na_2SO_4$ 0.5 mol $L^{-1}$ (a unique quasi-reversible system at 0.64 V *vs.* SCE).

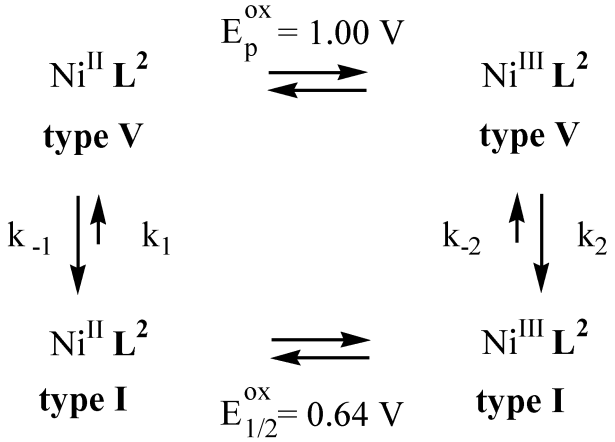


**Scheme 2** Oxidatively induced isomerisation of $[NiL^2]^{2+}$-type V into $[NiL^2]^{2+}$-type I complex.

The next point to check is if the coordination of the pyridine nitrogen atom remains in the course of the isomerisation process. For that, the cyclic voltammetry of $[Ni^{II}L^2]^{2+}$-type I in a very acidic medium was investigated and compared with the well known $[Ni^{II}L^3]^{2+}$-type III compound,† for which the metal coordination sphere is $NiN_4$.[20] Although the voltammogram in acidic medium is not well resolved, one can immediately see the similarity between the CV waves of both compounds ($Ni^{II/III}$ process occurs at the same potential 0.72 V *vs.* SCE, see Table 4): it means that under acidic conditions, the pyridine is no longer coordinated to the metal ion in the $[Ni^{II}L^2]^{2+}$-type I complex. So, in neutral conditions, where the isomerisation process between $Ni^{III}$-type V and $Ni^{III}$-type I isomers is observed, the pyridine coordination is kept. It is worth noting that in very acidic media, a third $[Ni^{II}L^2]^{2+}$ species exists, probably with a type III configuration, in which the pyridine nitrogen atom is protonated and therefore no longer coordinated to the metallic cation. Electron paramagnetic resonance can also provide information on the electron density distribution and coordination geometry of the metal ion in the oxidation products.[21] For that, since the square planar $Ni^{II}$ $d^8$ metallic ion is diamagnetic, the chemical oxidation previously described was used to generate the $Ni^{III}$ species. Whatever the starting complex (type I or type V), the anisotropic ESR spectra in water–glycerol at 150 K show axial symmetry with $g_\perp > g_\parallel$ and a value of $g_\perp$ considerably greater than 2 ($g_\perp = 2.172$, $g_\parallel = 2.032$, $A_\perp = 5.1 \times 10^{-4}$ $cm^{-1}$, $A_\parallel = 20.9 \times 10^{-4}$ $cm^{-1}$). In all cases, $g_\parallel$ is split into three lines with intensity ratio of 1 : 2 : 1. These observations are consistent with the existence of low spin $d^7$ $Ni^{III}$ complexes,[21] the superhyperfine splitting of the parallel signal confirming the coordination of the pyridine nitrogen atom in one of the axial positions.

The redox behaviour of the nickel cyclam complexes has also been investigated in acetonitrile solutions. Table 5 regroups the half wave potentials measured during this work. The $[Ni^{II}L^2]^{2+}$-type I and $[Ni^{II}L^2]^{2+}$-type V electrochemical behaviours are represented in Fig. 4. The oxidation of the pure

View Article Online

**Table 5** Redox potentials (V *vs.* $Fc^+/Fc$) of $[Ni^{II}L^2]^{2+}$-type I, $[Ni^{II}L^2]^{2+}$-type V and $[Ni^{II}L^3]^{2+}$-type III at a glassy carbon electrode in MeCN–$Bu_4NPF_6$ 0.1 mol $L^{-1}$

| Complex | $E_{\frac{1}{2}}^{ox}$ (V) *vs.* $Fc^+/Fc$ | $E_{\frac{1}{2}}^{red}$ (V) *vs.* $Fc^+/Fc$ |
|---|---|---|
| $[Ni^{II}(\mathbf{cyclam})]^{2+}$-type III | 0.64 ($\Delta E_p$ = 90 mV) | −1.79 ($\Delta E_p$ = 110 mV) |
| $[Ni^{II}L^2]^{2+}$-type I | 0.68 ($\Delta E_p$ = 90 mV) | −1.92 ($\Delta E_p$ = 90 mV) |
| $[Ni^{II}L^2]^{2+}$-type V | 1.01 ($\Delta E_p$ = 100 mV) | −1.92 ($\Delta E_p$ = 90 mV) |
| $[Ni^{II}L^3]^{2+}$-type III | 0.80 ($\Delta E_p$ = 90 mV) | −1.64 ($\Delta E_p$ = 90 mV) |

$[Ni^{II}L^2]^{2+}$-type I complex is quasi-reversible and occurs at 0.68 V *vs.* $Fc^+/Fc$ (Fig. 4a). For the $[Ni^{II}L^2]^{2+}$-type I complex, as long as the reduction is not investigated, the $Ni^{II/III}$ system is fully reproducible and occurs at $E_{\frac{1}{2}}$ = 0.68 V *vs.* $Fc^+/Fc$, which underlines the large stability of the $Ni^{III}$ complex formed. When the first scan is clipped towards negative potentials, the $Ni^{II}$ complex is quasi-reversibly reduced to $Ni^{I}$. When the potential is subsequently and immediately raised, the $Ni^{II}$ oxidation happens this time in two separate systems at 0.68 V *vs.* $Fc^+/Fc$ and at 1.01 V *vs.* $Fc^+/Fc$. These observations are in agreement with an equilibrium between the $[Ni^{I}L^2]^{+}$-type I isomer and another configuration of the complex, certainly the $[Ni^{I}L^2]^{+}$-type V one. Further scans carried on oxidation show the disappearing of the second oxidation system at 1.01 V. It is important to notice that there is no need to go back in oxidation to see the decrease of the second system: it naturally disappears when the potential is maintained at a value which gives zero current. It means that in the absence of water, the type V complex is rapidly interconverted into the type I complex.

Concerning the type V isomer (Fig. 4b), the oxidation is already separated into two waves, one at 0.68 V *vs.* $Fc^+/Fc$ and the other one at 1.01 V *vs.* $Fc^+/Fc$ and the voltammogram is preserved after several scans. After reduction no or few changes are observed in the whole potential range which means that, in this case, no redox isomerisation can be considered. It was not the case in the previous experiment in acetonitrile for the pure $[Ni^{II}L^2]^{2+}$-type I isomer.

To explain these discrepancies in acetonitrile solutions, one must consider that first, the elemental analysis of $[Ni^{II}L^2]^{2+}$-type I shows that the complex is strictly anhydrous and second, the type V isomer is monohydrated. Since the solvent used for the electrochemical measurements is strictly anhydrous, it signifies that water is necessary to stabilise the $Ni^{II/III}L^2$-type V form.[22]

## Conclusion

In conclusion, the investigations undertaken in the present work have shown that the presence of a pyridine pendant arm on a cyclam cavity allows the isolation of two configurational isomers for the nickel complex, respectively the $[NiL^2]^{2+}$-type I and the $[NiL^2]^{2+}$-type V. This is not the case for the corresponding cyclen complex probably because the cavity is less flexible. Concerning the $[NiL^2]^{2+}$-type I and -type V complexes, an isomerisation mechanism between these two configurations was established mostly by electrochemical experiments. These characterisations underlined that type V to type I isomerisation is favoured in water and kinetically faster with $Ni^{III}$. This result demonstrates the relevance of electron transfer in inducing geometrical reorganisations. According to electrochemical measurements, the type I isomer is thermodynamically more stable than the type V one. This equilibrium is disrupted in dry acetonitrile which means that the presence of water is necessary to improve the stability of the $Ni^{III}$ oxidation state of the type V kinetic isomer. Finally, in dry

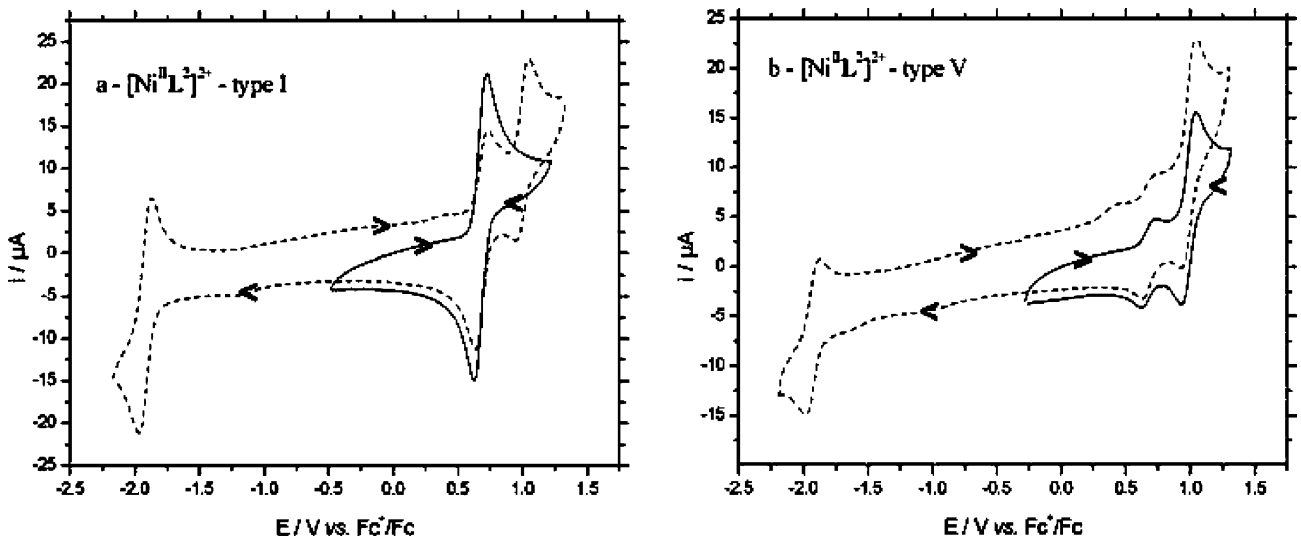


**Fig. 4** Cyclic voltammetry at a glassy carbon disk (100 mV $s^{-1}$) in MeCN–$Bu_4NPF_6$ 0.1 mol $L^{-1}$ of (a) $[Ni^{II}L^2]^{2+}$-type I (solid line: oxidation scan, dashed line: scan in reduction prior to oxidation) and (b) $[Ni^{II}L^2]^{2+}$-type V (solid line: oxidation scan, dashed line: scan in reduction prior to oxidation).

Downloaded by University of California - Los Angeles on 01 January 2013
Published on 20 January 2006 on http://pubs.rsc.org | doi:10.1039/B515107D

 This journal is © the Royal Society of Chemistry the Centre National de la Recherche Scientifique 2006

View Article Online

acetonitrile, isomerisation involving the $Ni^{I}$ oxidation state seems to occur.

## Experimental

### Syntheses

The metals salts were purchased from Aldrich. The other reagents were used as the highest grade commercially available without further purification.

**Ligands $L^1$ and $L^2$.** The ligands $L^1$ and $L^2$ have been synthesised according to the bis(aminal) methodology[9] by alkylation of cyclen or cyclam glyoxal ligands with (bromomethyl)pyridine (obtained according to ref. 23).

Ligand $L^1$ (yield; 85%): $\delta_C$ (67.8 MHz; $D_2O$): 43.2, 44.3, 45.0, 50.9 and 59.7 ($CH_2N$), 123.0, 124.5, 138.0, 148.0 and 158.3 ($C_{ar}$). Elemental analysis: found for $L^1$: C, 52.94; H, 9.96; N, 21.29%, calc. for $C_{14}H_{25}N_5 \cdot 0.25C_2H_5OH \cdot 3H_2O$: C, 52.69; H, 9.84; N, 21.59%;. ESI-MS ($m/z$): exp.: 264.1 (100%), calc. for $[L^1H]^+$: 264.2.

Ligand $L^2$ (yield; 86%): $\delta_C$ (67.8 MHz; $D_2O$): 24.9 and 26.9 ($CH_2CH_2N$), 45.6, 46.3, 46.7, 47.3, 47.5, 48.4, 53.6, 53.8 and 58.8 ($CH_2N$), 122.9, 123.9, 137.9, 147.9 and 158.7 ($C_{ar}$). Elemental analysis: found for $L^2$: C, 63.66; H, 10.04; N, 23.08%, calc. for $C_{16}H_{29}N_5 \cdot 0.5H_2O$: C, 63.95; H, 10.07; N, 23.32%; ESI-MS ($m/z$): exp.: 292.3 (100%), calc. for $[L^2H]^+$: 292.3.

**$[NiL^1(ClO_4)_2] \cdot 2H_2O$.** Nickel perchlorate hexahydrate (133 mg, 0.36 mmol) in methanol (5 mL) was added dropwise to $L^1$ (100 mg, 0.32 mmol) in methanol (15 mL). The purple solution was refluxed for 2 hours and the solution was concentrated by evaporation.

This solid was further dissolved in acetonitrile and the diffusion of a diethyl ether solution produced purple monocrystals of $[NiL^1(ClO_4)_2] \cdot 2H_2O$, suitable for X-ray analysis.

Elemental analysis: found: C, 30.44; H, 4.64; N, 12.38%, calc. for $C_{14}H_{25}N_5NiCl_2O_8 \cdot 2H_2O$: C, 30.27; H, 5.26; N, 12.61%; ESI-MS ($m/z$): exp.: 420.2 (60%), calc. for $[NiL^1(ClO_4)]^+$: 420.1; exp.: 320.2 (100%), calc. for $[NiL^1H_{-1}]^+$: 320.1.

**$[NiL^2(ClO_4)_2]$-type I and $[NiL^2(ClO_4)_2 \cdot 0.25H_2O]$-type V.** Nickel perchlorate hexahydrate (260 mg, 0.71 mmol) in methanol (5 mL) was added dropwise to $L^2$ (195 mg, 0.64 mmol) in methanol (15 mL). The purple solution was heated at reflux for one hour. The mixture was stirred at room temperature for one day, the pink precipitate was filtered and was dissolved in acetonitrile. Light pink crystals were obtained by slow diffusion of ether in the acetonitrile solution; complex (type I isomer) 27% yield.

Elemental analysis: found for $C_{16}H_{29}N_5NiCl_2O_8$: C, 35.03; H, 5.15; N, 12.52%; calc.: 35.00; H, 5.32; N, 12.75%. The filtrate was then concentrated and the purple crystals were obtained after slow evaporation (type V isomer). Elemental analysis: found: C, 34.58; H, 4.96; N, 12.43%, calc. for $C_{16}H_{29}N_5NiCl_2O_8 \cdot 0.25H_2O$: C, 34.72; H, 5.37; N, 12.65%; ESI-MS ($m/z$) for type I and V: exp.: 448.1 (70%), calc. for $[NiL^2(ClO_4)]^+$: 448.1; exp.: 348.1 (100%), calc. for $[NiL^2H_{-1}]^+$: 348.2.

**$[NiL^3(ClO_4)_2]$-type III.** This complex have been synthesised according to ref. 24.

### Spectroscopic measurements

$^{13}C$ NMR spectra were recorded on a Bruker AC 250 NMR spectrometer. Mass spectra in acetonitrile were recorded on a Micromass Q-TOF electrospray positive ionisation mass spectrometer. Electronic spectra in aqueous or acetonitrile solutions ($10^{-3}$ mol $L^{-1}$) and perchloric acid 5 mol $L^{-1}$ solution were all measured in the 300–900 nm range on a Lambda 6 Perkin Elmer spectrophotometer. ESR spectra of $[Ni^{III}L^2]^{3+}$-type I/V complexes were recorded at 150 K on a Bruker

**Table 6** Crystal data and details of the structure determination for $[NiL^{1,2}]^{2+}$ complexes

| | $[NiL^1(CH_3CN)](ClO_4)_2$ | $[NiL^2(CH_3CN)$-typeI$](ClO_4)_2 \cdot CH_3CN$ | $[NiL^2(H_2O)$-typeV$](ClO_4)_2$ |
|---|---|---|---|
| Empirical formula | $C_{16}H_{28}Cl_2N_6NiO_8$ | $C_{20}H_{35}Cl_2N_7NiO_8$ | $C_{16}H_{31}Cl_2N_5NiO_9$ |
| Formula weight | 562.05 | 631.15 | 567.05 |
| Temperature (K) | 120(2) | 120(2) | 120(2) |
| Crystal system | Orthorhombic | Monoclinic | Orthorhombic |
| Space group | *Pbca* | $P2_1$ | $P2_12_12_1$ |
| Colour | Violet | Colourless | Violet |
| $a$ (Å) | 14.6107(2) | 14.2314(11) | 9.4023(5) |
| $b$ (Å) | 14.6567(2) | 12.7251(11) | 15.7925(5) |
| $c$ (Å) | 21.6728(3) | 15.5407(12) | 16.3876(5) |
| $\alpha$ (°) | 90.000 | 90.000 | 90.000 |
| $\beta$ (°) | 90.000 | 98.313(4) | 90.000 |
| $\gamma$ (°) | 90.000 | 90.000 | 90.000 |
| Volume (Å$^3$) | 4641.11(11) | 2784.8(4) | 2433.3(2) |
| $Z$ | 8 | 4 | 4 |
| $D_{calc}$ (g cm$^{-3}$) | 1.609 | 1.505 | 1.549 |
| Absorption coefficient (mm$^{-1}$) | 1.121 | 0.944 | 1.073 |
| $F(000)$ | 2336 | 1320 | 1184 |
| $\lambda$ (Mo-K$\alpha$), (Å) | 0.71073 | 0.71073 | 0.71073 |
| N° independent reflns | 5290 | 11072 | 5541 |
| N° reflns [$I > 2.0\sigma(I)$] | 4300 | 8922 | 4325 |
| $R_1$ | 0.0370 | 0.1011 | 0.0435 |
| w$R_2$ | 0.0922 | 0.2002 | 0.108 |
| Goodness-of-fit on $F^2$ | 1.061 | 1.152 | 1.011 |

Published on 20 January 2006 on http://pubs.rsc.org | doi:10.1039/B515107D
Downloaded by University of California - Los Angeles on 01 January 2013

View Article Online

ESP300e spectrometer (X band, frequency $\approx$ 9.4 GHz) in a water–glycerol (90 : 10) solution to ensure a good glass. The spectra were simulated with the Simfonia program to calculate the $g$ and $A$ parameters.

### Electrochemical measurements

Voltammetric data were recorded on an Autolab with PGSTAT12 potentiostat (ECO Chemie) associated to a conventional three electrode electrochemical cell, the working electrode being a glassy carbon, a platinum plate being used as a counter electrode and in aqueous medium a saturated calomel electrode was used as the reference while in acetonitrile a silver electrode separated from the complex solution was used as a *pseudo* reference. In acetonitrile, the potential of the *pseudo* reference was measured *versus* the ferricinium/ferrocene couple. Complex concentrations were always close to $10^{-3}$ mol $L^{-1}$, the supporting electrolyte being in acetonitrile tetrabutylammonium hexafluorophosphate ($10^{-1}$ mol $L^{-1}$) and in aqueous solutions, sodium sulfate (0.5 mol $L^{-1}$).

### Crystal structure determination

The crystal diffraction data were collected at 120 K on a Kappa CCD diffractometer (Centre de Diffractométrie X, Univ. Rennes, France) using monochromated Mo-K$\alpha$ radiation ($\lambda = 0.71073$ Å). Data collection was performed with the COLLECT program.[25] Frames integration and data reduction procedures have been realised using the DENZO and SCALEPACK program of the KappaCCD software package, respectively[26] for the Ni$\mathbf{L^1}$ and Ni$\mathbf{L^2}$-type I/V compounds and with EVAL[27] and SADABS[28] programs. Selected data are given in Table 6.‡

The structures were solved using the direct methods program SIR97,[29] that revealed all non-hydrogen atoms. SHELXL97[30] has been used to refine the structure. Finally hydrogen atoms were placed geometrically and held in riding mode in the least-squares refinement procedure. Final difference maps revealed no significant maxima.

## References


1 (*a*) M. Meyer, V. Dahaoui-Gingrey, C. Lecomte and R. Guilard, *Coord. Chem. Rev.*, 1998, **178–180**, 1313; (*b*) J. Costamagna, G. Ferraudi, B. Matsuhiro, M. Campos-Vallette, J. Canales, M. Villagrán, J. Vargas and M. J. Aguirre, *Coord. Chem. Rev.*, 2000, **196**, 125.

2 (*a*) D. Parker, *Chem. Soc. Rev.*, 1990, **19**, 271; (*b*) S. Jurisson, D. Berning, W. Jia and D. Ma, *Chem. Rev.*, 1993, **93**, 1137; (*c*) V. Alexander, *Chem. Rev.*, 1995, **95**, 273.

3 (*a*) F. Barbette, F. Rascalou, H. Chollet, J. L. Bahoubot, F. Denat and R. Guilard, *Anal. Chim. Acta*, 2004, **502**, 179; (*b*) F. Cuenot, M. Meyer, A. Bucaille and R. Guilard, *J. Mol. Liq.*, 2005, **118**, 89.

4 (*a*) *The Chemistry of Contrast Agents in Medical Magnetic Resonance Imaging*, ed. A. E. Merbach and E. Tóth, Wiley, Chichester, 2001; (*b*) J. Moreau, E. Guillon, J. C. Pierrard, J. Rimbault, M. Port and M. Aplincourt, *Chem.–Eur. J.*, 2004, **10**, 5218.

5 L. Siegfried and T. A. Kaden, *Dalton Trans.*, 2005, 3079.

6 (*a*) F. Wuerthner and J. Rebek, *Angew. Chem., Int. Ed. Engl.*, 1995, **34**, 446; (*b*) J. M. Kern, L. Raehm, J. P. Sauvage, B. Divisia-Blohorn and P. L. Vidal, *Inorg. Chem.*, 2000, **39**, 1555; (*c*) R. Ballardini, V. Balzani, A. Credi, M. T. Gandolfi and M. Venturi, *Acc. Chem. Res.*, 2001, **34**, 445; (*d*) N. Armaroli, V. Balzani, J. P. Collin, P. Gavina, J. P. Sauvage and B. Ventura, *J. Am. Chem. Soc.*, 1999, **121**, 4397; (*e*) V. Amendola, L. Fabbrizzi, C. Mangano and P. Pallavicini, *Acc. Chem. Res.*, 2001, **34**, 488; (*f*) C. P. Collier, E. W. Wong, M. Belohradsky, F. M. Raymo, J. F. Stoddart, P. J. Kuekes, R. S. Williams and J. R. Heath, *Science*, 1999, **285**, 391.

7 (*a*) C. Amatore, J. M. Barbe, C. Bucher, E. Duval, R. Guilard and J. N. Verpaux, *Inorg. Chim. Acta*, 2003, 267; (*b*) C. Bucher, J. C. Moutet, J. Pécaut, G. Royal, E. Saint-Aman, F. Thomas, S. Torelli and M. Ungureanu, *Inorg. Chem.*, 2003, **42**, 2242; (*c*) C. Bucher, J. C. Moutet, J. Pécaut, G. Royal, E. Saint-Aman and F. Thomas, *Inorg. Chem.*, 2004, **43**, 3777.

8 (*a*) E. Kimura, Y. Kotake, T. Koike, M. Shionoya and M. Shiro, *Inorg. Chem.*, 1990, **29**, 4991; (*b*) D. T. Pierce, T. L. Hatfield, E. J. Billo and Y. Ping, *Inorg. Chem.*, 1997, **36**, 2950.

9 M. Le Baccon, F. Chuburu, L. Toupet, H. Handel, M. Soibinet, I. Déchamps-Olivier, J. P. Barbier and M. Aplincourt, *New J. Chem.*, 2001, **25**, 1168.

10 B. Bonisch, C. V. Poon and M. L. Tobe, *Inorg. Chem.*, 1965, **4**, 1102.

11 M. A. Donnelly and M. Zimmer, *Inorg. Chem.*, 1999, **38**, 1630.

12 V. J. Thöm, C. C. Fox, J. C. A. Boeyens and R. D. Hancock, *J. Am. Chem. Soc.*, 1984, **106**, 5947.

13 A. S. Batsanov, A. E. Goeta, J. A. K. Howard, D. Maffeo, H. Puschmann and J. A. G. Williams, *Polyhedron*, 2001, **20**, 981.

14 S. El Ghachtouli, C. Cadiou, I. Déchamps-Olivier, F. Chuburu, M. Aplincourt, V. Turcry, M. Le Baccon and H. Handel, *Eur. J. Inorg. Chem.*, 2005, 2658.

15 L. Sabatini and L. Fabbrizzi, *Inorg. Chem.*, 1979, **18**, 438.

16 G. J. Bridger, R. T. Skerlj, S. Padmanabhan, S. A. Martellucci, G. W. Henson, M. J. Abramo, H. C. Joao, M. Witvrouw, K. De Vreese, R. Pauwells and E. De Clercq, *J. Med. Chem.*, 1996, **39**, 109.

17 (*a*) A. Bencini, L. Fabbrizzi and A. Poggi, *Inorg. Chem.*, 1981, **20**, 2544; (*b*) A. Buttafava, L. Fabbrizzi, A. Perotti, A. Poggi, G. Poli and B. Seghi, *Inorg. Chem.*, 1986, **25**, 1456.

18 H. Raznoshik, I. Zilbermann, E. Maimon, A. Ellein, H. Cohen and D. Meyerstein, *Inorg. Chem.*, 2003, **42**, 7156.

19 D. B. Rorabacher, *Chem. Rev.*, 2004, **104**, 651.

20 Y. Dong, G. A. Lawrence, L. F. Lindoy and P. Turner, *Dalton Trans.*, 2003, 1567.

21 F. V. Lovecchio, E. S. Gore and D. H. Busch, *J. Am. Chem. Soc.*, 1974, **96**, 3109.

22 I. Zilbermann, E. Maimon, H. Cohen and D. Meyerstein, *Chem. Rev.*, 2005, **105**, 2609.

23 A. E. Goeta, J. A. K. Howard, D. Maffeo, H. Puschmann, J. A. G. Williams and D. S. Yufit, *J. Chem. Soc., Dalton Trans.*, 2000, 1873.

24 Y. Dong, L. F. Lindoy, P. Turner and G. Wey, *Dalton Trans.*, 2004, 1264.

25 COLLECT: KappaCCD software, Nonius BV, Delft, The Netherlands, 1998.

26 Z. Otwinowski and W. Minor, in *Methods in Enzymology*, ed. C. W. Carter Jr and R. M. Sweet, Academic Press, New York, 1997, vol. 276, p. 307.

27 A. Altomare, M. C. Burla, M. Camalli, G. Cascarano, C. Giacovazzo, A. Guagliardi, A. G. G. Moliterni, G. Polidori and R. Spagna, *J. Appl. Crystallogr.*, 1999, **32**, 115.

28 G. M. Sheldrick, *SADABS version 2.03.*, Bruker AXS Inc., Madison, Wisconsin, USA, 2002.

29 A. J. M. Duisenberg, *Reflections on Area detectors*, PhD thesis, Utrecht University, 1998.

30 G. M. Sheldrick, *SHELXL-97, Program for refinement of crystal structures*, University of Göttingen, Germany, 1997.


‡ CCDC reference numbers 293319–293321. For crystallographic data in CIF or other electronic format see DOI: 10.1039/b515107d

Published on 20 January 2006 on http://pubs.rsc.org | doi:10.1039/B515107D
Downloaded by University of California - Los Angeles on 01 January 2013

 This journal is © the Royal Society of Chemistry the Centre National de la Recherche Scientifique 2006